

Edge Detection Techniques in Digital and Optical Image Processing

P. Bhuvaneshwari¹, Dr. A. Brintha Therese²

¹(Asso. Professor, Department of Electronics & Communication Engg, RRCE Bangalore & Research Scholar, VIT University, Chennai)

² (Professor, SENSE Department, VIT University, Chennai)

ABSTRACT

This study focuses on various edge detection methods. Edge detection is the common approach used in segmentation. In an image, edge can be the boundary between two regions with relatively distinct grey level properties. Edge detection is the most familiar approach used in medical field, vehicle parking management system etc for segmentation. The aim of this paper is studying different edge detection methods employed in digital image processing like, Robert, Sobel, Prewitt, Canny edge detection and bipolar edge detection which is based on optical image processing. The experimental results are obtained using MATLAB software and displayed.

Keywords: Bipolar incoherent image processing Robert, Sobel Prewitt, Canny, edge detection

I. INTRODUCTION

Visual information plays an important role in many aspects of our life. Image processing is a sequence of operations which are applied to the images to enhance, alter, or select regions of interest (segmentation). Several techniques have been proposed for automatic segmentation in medical images, such as thresholding, edge detection, region growing, and morphological operations. In the present scenario imaging is one of the most useful diagnostic tools available in medical field [1]. In imaging the pre-processing step plays a vital role especially in segmentation. Edge detection filters are used in this case. These filters are used in the process of identifying the image by locating the sharp edges which are discontinuous. These discontinuities bring changes in pixels intensities which define the boundaries of the object [2]. In this paper the implementation of several edge detection filters existing in digital image processing and optical image processing are discussed. A brain image is taken as an example and the results are displayed. These methods are tested with various images also. This paper is organized as follows: Section 2 deals with the theory behind the optical and digital image processing techniques, followed by section 3 in which various edge detection filters are discussed. In section 4 experimental results are shown and section 5 deals with the findings of the study.

II. RELATED WORK

2.1 Optical Image Processing

Optical Image Processing has been proposed as a method for dealing with massive data that has become increasingly sophisticated year by year.

Conventional electronic computers have sequential processing whereas Optical Image Processing enables us to deal with the image information in parallel, which can offer dramatic improvement in the processing speed of image information [3]. The maximum resolution is achievable which is in digital image processing limited by the density of pixels. It is possible to implement optical image processing even in the case of relatively low beam intensity using the high non linearity of the Photo Refractive effect.

2.2 Digital Image Processing

Processing of images by means of digital computer which means that the image information is calculated pixel by pixel. It allows a much wider range of algorithms to be applied to the input data and can avoid problems such as the build-up of noise and signal distortion during processing since images are defined systems. The principle advantage of Digital Image Processing methods is its versatility, repeatability and the preservation of original data precision.

III. PROPOSED WORK

3.1 Bipolar incoherent edge detection (optical)

This is an optical edge detection method. Using band pass filtering the edge is detected. An Acousto Optic Heterodyning Image Processing (AOHIP) system which is a two pupil system shown in Fig 3.1 is used. The band pass filter is tuned at heterodyne frequency Ω , and PMT is a photomultiplier for the detection of scattered light from the 3-D object. Beamsplitters BS and BS1, and mirrors M and M1 form the Mach-Zehnder

interferometer. A collimated laser at temporal frequency ω_0 is used to illuminate the pupil, $P_1(x, y)$. The other pupil, $P_2(x, y)$, is illuminated by the laser of temporal frequency $\omega_0 + \Omega$. The laser's temporal frequency offset of Ω is introduced by an acousto-optic frequency shifter (AOFS) as shown in the Figure 3.1. The two pupils are located at the front focal planes of lens L_1 and L_2 , both with focal length f . The two pupils are then combined by beam splitter BS1 to focus the light onto the 2-D $x - y$ scanning mirrors, which are located on the back focal plane of lenses L_1 and L_2 . The combined optical scanning field at z away from the focal plane of the two lenses is then given by

$$P_{1z}(k_0x/f, k_0y/f) \exp(j\omega_0 t) + P_{2z}(k_0x/f, k_0y/f) \exp[j(\omega_0 + \Omega)t],$$

Where $P_{1z}(k_0x/f, k_0y/f)$ are the field distribution z away from the mirrors M_1 and M_2

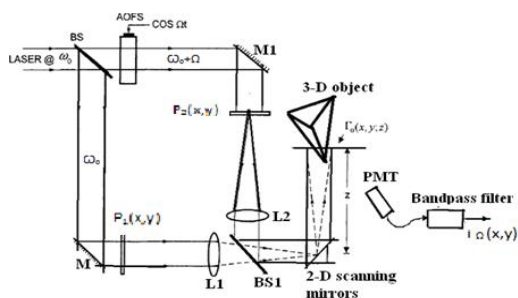


Fig 3.1AOHIP System

The combined optical field or the scanning pattern is used to perform a two dimensional scan of a 3-D object using the 2-D scanning mirrors. We now model the 3-D object as a collection of planar amplitude distribution $\Gamma_o(x, y; z)$ along its depth direction, z . z is a depth parameter which is measured away from the scanning mirrors as shown in Figure 3.1. The photomultiplier (PMT), which responds to the incident intensity of the optical transmitted field or scattered field, generates a current that is given by

$$i(x, y; z) = \iint_A | [P_{1z} \left(\frac{k_0x'}{f}, \frac{k_0y'}{f} \right) e^{j(\omega_0 t)} + P_{2z} \left(\frac{k_0x'}{f}, \frac{k_0y'}{f} \right) e^{j(\omega_0 + \Omega)t}] \times \Gamma_o(x + x', y + y'; z) |^2 dx' dy' \quad (3.1)$$

The shifted coordinates of Γ_o represent the action of scanning. The heterodyne current at temporal frequency Ω of Eq. (3.1), after a band pass filter tuned at frequency Ω , becomes

$$i_\Omega(x, y; z) = \text{Re} \left[\iint_A P_{1z}^* \left(\frac{k_0x'}{f}, \frac{k_0y'}{f} \right) P_{2z} \left(\frac{k_0x'}{f}, \frac{k_0y'}{f} \right) \Gamma_o(x + x', y + y'; z) dx' dy' \exp(j\Omega t) \right] \quad (3.2)$$

$$i_\Omega(x, y) = \text{Re} [i_{\Omega p}(x, y; z) \exp(j\Omega t)] \quad (3.3)$$

We shall now define optical transfer function (OTF) of the system as

$$OTF_\Omega(k_x, k_y; z) = \mathcal{F} \{ i_{\Omega p}(x, y; z) \} / \mathcal{F} \{ |\Gamma_o(x, y; z)|^2 \} \quad (3.4)$$

Substituting Eq.3.2 into Eq.3.3 we have

$$OTF_\Omega(k_x, k_y; z) = \mathcal{F}^* \left\{ P_{1z} \left(\frac{k_0x}{f}, \frac{k_0y}{f} \right) P_{2z}^* \left(\frac{k_0x}{f}, \frac{k_0y}{f} \right) \right. \\ \left. \exp \left[j \frac{z}{2k_0} (k_x^2 + k_y^2) \right] \right\} \times \iint p_1^*(x', y') p_2 \left(x' + \frac{f}{k_0} k_x, y' + \frac{f}{k_0} k_y \right) \exp \left[\frac{jz}{f} (x' k_x + y' k_y) \right] dx' dy' \quad (3.6)$$

$$OTF_\Omega(k_x, k_y; z) = \exp \left[j \frac{z}{2k_0} (k_x^2 + k_y^2) \right] \times \iint p_1^*(x', y') p_2 \left(x' + \frac{f}{k_0} k_x, y' + \frac{f}{k_0} k_y \right) \exp \left[\frac{jz}{f} (x' k_x + y' k_y) \right] dx' dy' \quad (3.6)$$

This Equation states that OTF_Ω

$$i_\Omega(x, y; z) = \text{RE} [i_{\Omega p}(x, y; z) \exp(j\Omega t)] \quad (3.7)$$

$$= \text{Re} \left[\mathcal{F}^{-1} \{ \mathcal{F} \{ |\Gamma_o(x, y; z)|^2 \} \} OTF_\Omega(k_x, k_y; z) \right] \exp(j\Omega t) \quad (3.8)$$

Defining the point spread function of optical heterodyne scanning system as

$$h_\Omega(x, y; z) = \mathcal{F}^{-1}(OTF_\Omega) \quad (3.9)$$

$$i_\Omega(x, y; z) = \text{Re} [|\Gamma_o(x, y; z)|^2 \otimes h_\Omega(x, y; z) \exp(j\Omega t)] \quad (3.10)$$

Equation (3.7) or(3.10) represents the scanned and processed output current modulated by temporal carrier at frequency Ω . We can demodulate and extract the in-phase and the quadrature components of the output current by mixing it with $\cos(\Omega t)$ and $\sin(\Omega t)$,

$$i_c(x, y; z) = \text{Re} \left[\mathcal{F}^{-1} \{ \mathcal{F} \{ |\Gamma_o(x, y; z)|^2 \} \} OTF_\Omega(k_x, k_y; z) \right] \\ = \text{Re} [|\Gamma_o(x, y; z)|^2 \otimes h_\Omega(x, y; z)] \quad (3.11)$$

$$i_s(x, y; z) = \text{Im} \left[\mathcal{F}^{-1} \{ \mathcal{F} \{ |\Gamma_o(x, y; z)|^2 \} \} OTF_\Omega(k_x, k_y; z) \right] \\ = \text{Im} [|\Gamma_o(x, y; z)|^2 \otimes h_\Omega(x, y; z)] \quad (3.12)$$

We assume that the object is now a 2-D Image and placed at focal plane of lenses L1 and L2. Hence $\Gamma_o(x, y; z)$ becomes $\Gamma_o(x, y; 0) = \Gamma_o(x, y)$

With the 2-D scanning mirrors moved towards the lenses for scanning purposes. We know as an example modifies Eq. (3.11) to clarify the idea of bipolar image processing. By setting $z = 0$ in Eq. (3.11), we have

$$i_c(x, y) = \text{Re} \left\{ \mathcal{F}^{-1} \left\{ \left[|\Gamma_o(x, y)|^2 \right] \text{OTF}_\Omega(k_x, k_y) \right\} \right\} = \text{Re} \left[|\Gamma_o(x, y)|^2 \otimes h_\Omega(x, y) \right] \quad (3.13)$$

Where $\text{OTF}_\Omega(k_x, k_y)$ becomes according to equ.

$$\text{OTF}_\Omega(k_x, k_y) = \iint p_1(x', y') p_2 \left(x' + \frac{f}{k_o} k_x, y' + \frac{f}{k_o} k_y \right) dx' dy' \quad (3.14)$$

And

$$h_\Omega(x, y) = \mathcal{F}^{-1} \left\{ \text{OTF}_\Omega(k_x, k_y) \right\} \quad (3.15)$$

Note that the OTF achievable is no longer the autocorrelation of the pupil function, but the cross correlation of the two pupils in the incoherent optical system, and hence the point spread function (PSF) becomes bipolar- the very concept of bipolar incoherent image processing. For simulation purposes, we take

$$P_1(x, y) = \exp[-a_1(x^2 + y^2)] - \exp[-a_2(x^2 + y^2)] \quad (3.16)$$

Difference-of-Gaussian aperture function (which is an annular-type pupil), and

$$P_2(x, y) = \delta(x, y) \quad (3.17)$$

a small pin-hole aperture. The OTF then becomes, using Eq. (3.14)

$$\text{OTF}_\Omega(k_x, k_y) = e^{-\sigma_1(k_x^2 + k_y^2)} - e^{-\sigma_2(k_x^2 + k_y^2)} \quad (3.18)$$

Where $\sigma_1 = a_1 \left(\frac{f}{k_o} \right)^2$ And $\sigma_2 = a_2 \left(\frac{f}{k_o} \right)^2$

This OTF is a band pass filtering function and according to Eq.(3.11), the spectrum of the intensity object, $|\Gamma_o(x, y; z)|^2$ is modified by this bandpass filtering action. The MATLAB code used to simulate bipolar incoherent filtering and the results are shown in Figure 4.1, Figure 4.1 (a) is the input image and Figure 4.1 (b) is its Fourier transform. Figure 4.1(c) shows the Difference-of-Gaussian OTF with chosen σ_1 and σ_2 . Finally, Figure 4.1 (d) shows the processed image, which clearly demonstrates edge extraction on the incoherent image.[4]

3.2 Classical Edge detection Operators (Digital)

There are many methods employed for edge detection in image processing, but most of them can be grouped into two categories, Gradient based search method and Laplacian based zero-crossing method. The gradient-based methods detect edges by first computing a measure of edge strength, usually a first-order derivative expression such as the gradient magnitude, and then searching for local directional maxima of the gradient magnitude using a computed estimate of the local orientation of the edge, usually the gradient direction. Here we are discussing Robert, Sobel and Prewitt edge operators under Gradient based edge detection. The zero-crossing based methods search for zero crossings in a second-order derivative expression computed from the image in order to find edges [5]. Canny operator has been discussed under the category of zero crossing. As a pre-processing step to edge detection, a smoothing stage, typically Gaussian smoothing, is applied [6].

3.2.1 Search-based (Gradient) edge detection

The gradient method detects the edges by looking for the maximum and minimum in the first derivative of the image [7]. Here some of the gradient based edge detectors Robert, Sobel and Prewitt are discussed.

A) Robert Edge detector

The Roberts operator performs a simple, quick to compute, 2-D spatial gradient measurement on an image. It thus highlights regions of high spatial gradient which often correspond to edges. In its most common usage, the input to the operator is a grayscale image, as is the output. Pixel values at each point in the output represent the estimated absolute magnitude of the spatial gradient of the input image at that point.

In theory, the operator consists of a pair of 2x2 convolution masks as shown in Figure 3.2.1

One mask is simply the other rotated by 90°. This is very similar to the Sobel operator.

| | |
|----|---|
| 0 | 1 |
| -1 | 0 |

Sx

| | |
|---|----|
| 1 | 0 |
| 0 | -1 |

Sy

Fig 3.2.1 (A) Roberts Cross convolution masks

These masks are designed to respond maximally to edges running at 45° to the pixel grid, one mask for each of the two perpendicular orientations. The masks can be applied separately to the input image, to produce separate measurements of the gradient component in each orientation (call these Sx and Sy). These can then be combined together to

find the absolute magnitude of the gradient at each point and the orientation of that gradient. The gradient magnitude is given by:

$$|S| = \sqrt{S_x^2 + S_y^2}$$

an approximate magnitude is computed using:

$$|S| = |S_x| + |S_y|$$

which is much faster to compute.

The angle of orientation of the edge giving rise to the spatial gradient (relative to the pixel grid orientation) is given by:

$$\theta = \arctan(S_y/S_x) - 3\pi/4$$

In this case, orientation θ is taken to mean that the direction of maximum contrast from black to white runs from left to right on the image, and other angles are measured anticlockwise[8].

B) Sobel edge detection operator

Sobel operator is a discrete differentiation operator used to compute an approximation of the gradient of image intensity function for edge detection. At each pixel of an image, sobel operator gives either the corresponding gradient vector or normal to the vector. It convolves the input image with kernel and computes the gradient magnitude and direction. It uses following 3x3 two kernel.

| | | |
|----|----|----|
| 1 | 2 | 1 |
| 0 | 0 | 0 |
| -1 | -2 | -1 |

S_x

| | | |
|----|----|----|
| 1 | 2 | 1 |
| 0 | 0 | 0 |
| -1 | -2 | -1 |

S_y

Fig 3.2.1(B) Sobel Cross convolution masks

As compared to Robert operator have slow computation ability but as it has large kernel so it is less sensitive to noise as compared to Robert operator. As having larger mask, errors due to effects of noise are reduced by local averaging within the neighborhood of the mask.

The gradient magnitude is given by:

$$|S| = \sqrt{S_x^2 + S_y^2}$$

an approximate magnitude is computed using:

$$|S| = |S_x| + |S_y|$$

which is much faster to compute.

The angle of orientation of the edge giving rise to the spatial gradient (relative to the pixel grid orientation) is given by:

$$\theta = \arctan(S_y/S_x)$$

C) Prewitt edge detection operator

The function of Prewitt edge detector is almost same as of sobel detector but have different Kernels[9]

| | | |
|----|---|----|
| -1 | 0 | 1 |
| -1 | 0 | 1 |
| -1 | 0 | -1 |

S_x

| | | |
|----|----|----|
| 1 | 1 | 1 |
| 0 | 0 | 0 |
| -1 | -1 | -1 |

S_y

Fig 3.2.1(C) Prewitt Cross convolution masks

Prewitt edge operator gives better performance than that of sobel operator.

3.2.2 Zero Crossing edge detector

The zero crossing detector looks for places in the Laplacian of an image where the value of the Laplacian passes through zero points where the Laplacian changes sign. Such points often occur at 'edges' in images points where the intensity of the image changes rapidly, but they also occur at places that are not as easy to associate with edges.

Zero crossings always lie on closed contours and so the output from the zero crossing detector is usually a binary image with single pixel thickness lines showing the positions of the zero crossing points.

The starting point for the zero crossing detector is an image which has been filtered using the Laplacian of Gaussian filter. The zero crossings that result are strongly influenced by the size of the Gaussian used for the smoothing stage of this operator.

A) Canny edge detection operator

Canny operator is a result of solving an optimization problem with constraints. The canny edge detection algorithm is known as the optimal edge detection. The Canny's intentions were to enhance all the edges acquiring in images[10].

The steps involved in Canny algorithm is explained through flowchart given below.

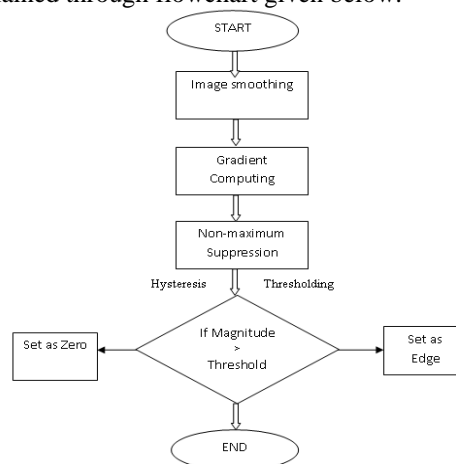


Fig3.2.2 Flow chart for canny edge detection

IV. EXPERIMENTAL RESULTS

A brain image is taken as an input image and the edges are detected using various detectors. The experimental result using matlab software is shown below

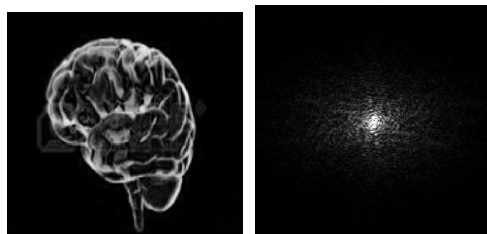


Fig 4.1(a) Fig 4.1(b)

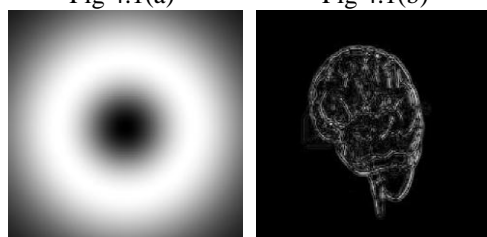


Fig 4.1(c) Fig 4.1(d)

Fig 4.1 Bipolar incoherent edge detector
 (a) Input image (b) Fourier Transform image (c) Difference-of-Gaussian OTF image (d) Edge detected image



Fig 4.2(a) Fig 4.2(b)

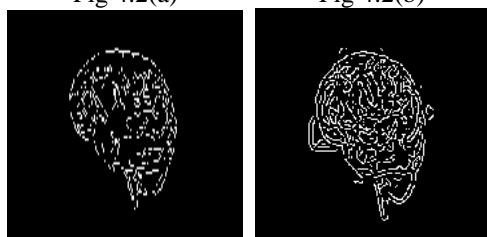


Fig 4.2(c) Fig 4.2(d)

Fig 4.2 Classical Edge detection Operators
 (a) Robert (b) Sobel (c) Prewit (d) Canny

In optical based edge detection the edges are detected precisely also the processing speed is much faster than other methods. This is the primary advantage of optical image processing. Classical operators like Robert, Sobel and prewitt are very simple due to the approximation of the gradient magnitude, but they are sensitive to noise hence expected accuracy will not be obtained. Canny operator gives better performance and each and every edge is detected.

V. CONCLUSION

In this paper various edge detection methods employed in digital and optical image processing are discussed and compared based on accuracy, processing speed, and noise .A brain image is considered and the experimental results are obtained using matlab software. Above mentioned edge detection methods were tested with various images also.

REFERENCES

- [1] Brintha Therese and Dr. Sundara vadivelu, Biploar incoherent image processing for edge detection, *International journal of recent trends in engineering Vol 2, No 2, 2009*
- [2] G. T. Shrivakshan and Dr. C. Chandrasekar, A comparison of various edge detection techniques used in image processing, *International journal of computer science issues ,Vol 9, Issue 5, No 1, 2012*
- [3] Daisuke Ishikawa, Atsushi Okamoto, All optical multifunctional logic gates for image information using photorefractive two wave mixing, *Optical Review, Vol 14, pp.246-251, 2007*
- [4] T. C. Poon ,Optical image processing with matlab, *springer-verlag, New York, first edition, 2007*
- [5] Dr. Vipula Singh, Digital image processing with matlab and labview(*Elsevier, 2013*)
- [6] Huertas.A and Medioni.G Detection of intensity changes with sub pixel accuracy using Laplacian –Gaussian masks, *IEEE Trans.on pattern Analysis and Machine Intelligence, vol 8, pp651-664, 1986*
- [7] Nick Kanopoulos, et al, Design of an image edge detection filter using sobel operator ,*Journal of solid state circuits IEEE vol 23, issue 2, pp.358-367, 1988*
- [8] Mamta Juneja and Parvinder Singh Sandhu , Performance evaluation of edge detection techniques for images in spatial domain, *International journal of computer theory and engineering, vol 1, No 5, 2009*
- [9] R.C. Gonzalez and R .E. Woods, Digital image processing, 2nd edition (*prentice Hall, 2002*)
- [10] Canny J, A computational approach to edge detection ,*IEEE Trans. pattern analysis and machine intelligence, vol 8, pp679-714, 1986*